frontiers | Frontiers in Energy Research

ORIGINAL RESEARCH
published: 17 June 2022
doi: 10.3389/fenrg.2022.890095

Vertical Protection Level Optimization and Availability Analysis for Advanced RAIM

Ershen Wang[1,2], *Wansen Shu*[1], *Xidan Deng*[1], *Zhi Wang*[3,4]*, *Song Xu*[1] *and Huan Wang*[1]

[1]School of Electronic and Information Engineering, Shenyang Aerospace University, Shenyang, China, [2]Liaoning General Aviation Academy, Shenyang Aerospace University, Shenyang, China, [3]Zhejiang Key Laboratory of General Aviation Operation Technology, Jiande, China, [4]CAAC Key Laboratory of General Aviation Operation, Department of General Aviation, Civil Aviation Management Institute of China, Beijing, China

With the introduction of global navigation satellite systems (GNSSs) in aviation, there has been increased dependency on GNSS position. Multi-constellation GNSS services and equipment will remain a solution for many aircraft positions in safety. Multi-constellation GNSS can improve robustness and navigation performance. Therefore, advanced receiver autonomous integrity monitoring (advanced RAIM or ARAIM) technology is being developed as an augmentation method for GNSS users under multi-constellation. ARAIM can allow increased service level globally and provide vertical guidance during the approach phase for aircrafts. Since the traditional ARAIM algorithm uses the average allocation strategy to allocate integrity and continuity risk, an allocation approach based on the particle swarm optimization (PSO) algorithm is presented in this article. Different allocation strategies for integrity and continuity risk are chosen as different particles, and the weighted sum of vertical protection level corresponding to different fault subsets is selected as the fitness function to optimize the allocation strategy and the corresponding VPL. Based on real GNSS data, the ARAIM algorithm under multi-constellation is analyzed. The experimental results demonstrate that the integrity and continuity risk allocation method based on the proposed algorithm optimizes the VPL and improves the global availability of ARAIM under multi-constellation.

Keywords: global navigation satellite system (GNSS), advanced RAIM, vertical protection level (VPL), availability analysis, particle swarm optimization (PSO) algorithm

OPEN ACCESS

Edited by:
Sudhakar Babu Thanikanti, Chaitanya Bharathi Institute of Technology, India

Reviewed by:
Xingqun Zhan, Shanghai Jiao Tong University, China
Rong Wang, Nanjing University of Aeronautics and Astronautics, China

***Correspondence:**
Zhi Wang
wangzhi@camic.cn

Specialty section:
This article was submitted to Smart Grids, a section of the journal Frontiers in Energy Research

Received: *10 March 2022*
Accepted: *09 May 2022*
Published: *17 June 2022*

Citation:
Wang E, Shu W, Deng X, Wang Z, Xu S and Wang H (2022) Vertical Protection Level Optimization and Availability Analysis for Advanced RAIM. Front. Energy Res. 10:890095. doi: 10.3389/fenrg.2022.890095

1 INTRODUCTION

With the development technologies and GNSS (Yi et al., 2022), the receiver autonomous integrity monitoring algorithm (RAIM) can provide aviation users with integrity monitoring in a non-precision approach phase under a single satellite navigation constellation and single fault (Wang et al., 2020). Integrity is a measure of trust that is used to determine whether the positing results provided by the navigation system is correct (Zhai et al., 2019b; Zhai et al.,2019c). The advanced receiver autonomous integrity monitoring (ARAIM) algorithm was proposed in the GNSS Evolutionary Architecture Study (GEAS) report which was developed to provide localizer precision with vertical guidance down to 200 feet altitude (LPV-200) for worldwide aircraft landing navigation (Blanch et al., 2012). ARAIM is an extension of the existing RAIM by adding more elements for the airborne integrity monitoring (Meng et al., 2019). The ARAIM receiver can receive navigation signals from multi-GNSS systems, and according to the integrity

support message (ISM) provided by ground monitoring stations, the fault subsets to be monitored and the probability of the corresponding monitoring subset are determined. The position estimation and integrity boundary of each subset are calculated by user segment, so the fault measurement value is identified and eliminated, and the protection level of the positioning solution is obtained (Bang et al.,2018; Bang et al.,2020; Wang E et al., 2020). At present, the research on ARAIM is focused on meeting the need for localizer performance with vertical guidance down to 200 feet altitude. (Joerger and Pervan, 2016; Joerger and Pervan, 2020)

Multi-constellation integrated navigation can improve the availability of ARAIM under LPV-200. At present, some scholars have proposed the ARAIM algorithm based on the combination of the BeiDou Navigation Satellite System (BDS), Galileo, and global positioning system (GPS) to improve the availability of ARAIM under LPV-200 navigation service. The current multipath error model in the ARAIM algorithm is based on data of GPS medium Earth orbit (MEO) satellites. The BDS constellation is different from the GPS; a BDS GEO satellite multipath effect for GNSS integrity monitoring in civil aviation is analyzed. The results show that the current error model in the ARAIM algorithm is no longer able to conservatively estimate the statistical characteristics of GEO satellites (Chang et al., 2021). To characterize BDS signal-in-space performance, some scholars provided a data-driven SISRE evaluation scheme by evaluating the overabounding user range accuracy (URA) and the prior fault probability to, respectively, capture the nominal and anomalous SIS behaviors (Wang E. et al., 2021). Zhai et al. (2019a) provided a novel integrity monitoring scheme by establishing the mechanism for determining the exclusion subset based on the projection magnitudes, and the results show that the new fault detection and exclusion (FDE) scheme can efficiently exclude the faulty satellites. Bang and Milner (2021) provided a new method by conducting H-ARAIM availability simulations, and examined the impact of the modified risk allocation on the existing fault detection and exclusion algorithm. Bang et al. (2018) studied the impact of the ARAIM fault detection test and the time correlation of position error on the probability of hazardously misleading information (PHMI), and proposed a method to estimate the actual PHMI within a given time interval to improve the availability of ARAIM. Zhao et al. (2020) provided a new method that establishes a direct relationship between mean estimation error and RB (residual-based) test statistic non-centrality parameter. The results show that the new method is about 6.9% higher than the SS-ARAIM. El-Mowafy and Yang. (2016) used real data to analyze ARAIM availability by collecting from 60 stations across Australia. Some scholars analyzed the influence of satellite geometrical distribution on integrity, reduced integrity risks under the premise of ensuring continuity risks, and analyzed the availability of ARAIM (Sun et al., 2015). These improvements optimize protection levels to some extent and improve the availability of ARAIM. In addition, the VPL is affected by the probability of hazardously misleading Information (PHMI) and probability of false alarm (PFA). In the traditional ARAIM algorithm, PHMI and PFA are evenly distributed to each fault subset. The different distributions of satellite orbit and different constellations will contribute to the positioning error; the average allocation strategy will affect the VPL and does not guarantee the optimal VPL. To solve this problem, some scholars studied the allocation of PHMI and PFA in the ARAIM algorithm, and then proposed an allocation method among the fault modes to obtain the minimum protection level per satellite geometry (Zhang et al., 2020). The availability of the ARAIM algorithm based on PHMI and PFA assignment problem was researched, and PHMI and PFA are evenly allocated to all fault subsets in the ARAIM algorithms (Working Group C, EU-U.S, 2016).

However, each fault subset of PHMI and PFA will affect the corresponding VPL. In this article, the PSO algorithm is combined with the PHMI and PFA allocation process. By optimizing the VPL, the proposed algorithm is analyzed and verified on the global VPL and availability of ARAIM based on multi-constellation GNSSs. The detailed processes of the proposed algorithm are provided. The results show that the optimized allocation method can optimize the VPL in different phases of aviation navigation and improve the global availability of ARAIM based on dual-constellation and multi-constellation GNSSs.

2 PROBLEM DESCRIPTION

ARAIM aims to realize global service with LPV-200 performance. The performance requirements for the LPV-200 service used to evaluate the availability of ARAIM are in line with the literature (Working Group C EU-U.S, 2017). The availability of ARAIM can be improved by optimizing the VPL.

Vertical Protection Level Calculation Method

The traditional ARAIM algorithm calculates the protection level (PL) according to the integrity requirements of the navigation system during the different flight phases. The VPL calculation based on the multiple hypothesis solution separation (MHSS) algorithm can be expressed as (Kropp et al., 2014):

$$VPL = max\left(VPL_0, VPL_k\right) \tag{1}$$

where VPL_k is the VPL corresponding to the fault subset k and $k = 0$ is the VPL corresponding to the fault-free subset (Blanch et al., 2014):

$$VPL_0 = K_{\mathrm{md},0} \times \sigma_{\mathrm{v},0} + \sum_{i=1}^{N_{\mathrm{sat}}} |S_0(3,i)| \times b_{\mathrm{nom},i} \tag{2}$$

$$VPL_k = D_k + K_{\mathrm{md},k} \times \sigma_{v,k} + \sum_{i=1}^{N_{\mathrm{sat}}} |S_k(3,i)| \times b_{\mathrm{nom},i} \tag{3}$$

where S_0 is the weighted least-squares projection matrix of the fault-free subset, S_k is the weighted least-squares matrix of the k fault subset, $b_{nom,i}$ is the maximum standard deviation of the satellite i used to evaluate the integrity, and D_k is the detection threshold corresponding to the k fault subset (Mei et al., 2017), expressed as:

$$D_k = K_{\mathrm{fa},k} \times \sigma_{\mathrm{dv},k} + \sum_{i=1}^{N_{\mathrm{sat}}} |\triangle \boldsymbol{S}_k(3,i)| \times b_{\mathrm{cont},i} \tag{4}$$

$$\triangle \boldsymbol{S}_k = \boldsymbol{S}_k - \boldsymbol{S}_0 \tag{5}$$

where

$$S_0 = \left(G^T \mathrm{WG}\right)^{-1} G^T W \tag{6}$$

$$S_k = \left(G^T M_k \mathrm{WG}\right)^{-1} G^T M_k W \tag{7}$$

G is the observation matrix and M_k is the identity matrix that the $k-th$ diagonal element is zeros. W is the weighting matrix, and $b_{\mathrm{cont},i}$ is the maximum standard deviation of the satellite i used to evaluate accuracy and continuity. In **Eqs 2–4**, $\sigma_{v,0}, \sigma_{v,k}$, and $\sigma_{dv,k}$ are the standard deviations of the detection statistics of the corresponding fault subset in the vertical direction, where

$$\begin{aligned} \sigma_{v,0} &= \sqrt{\left(G\mathrm{WG}^T\right)^{-1}_{3,3}} \\ \sigma_{v,k} &= \sqrt{\left(G^T M_k \mathrm{WG}\right)^{-1}_{3,3}} \\ \sigma_{dv,k} &= \sqrt{\left(\Delta S_k W^{-1} \Delta S_k^T\right)_{3,3}} \end{aligned} \tag{8}$$

The basic ARAIM algorithm uses the method of average allocation to allocate the coefficients. The continuity risk probability and integrity risk are evenly allocated to all satellites. $K_{\mathrm{md},k}$ and $K_{\mathrm{fa},k}$ are determined by $PHMI$ and PFA, expressed as follows:

$$\begin{aligned} K_{fa,0} &= 0 \\ K_{\mathrm{fa},k} &= -Q^{-1}\left(\frac{PFA}{N_{\mathrm{set}}}\right) \\ K_{\mathrm{md},0} &= -Q^{-1}\left(\frac{PHMI}{2\left(N_{\mathrm{set}}+1\right)}\right) \\ K_{md,k} &= -Q^{-1}\left(\frac{PHMI}{P_{sat,i}\left(N_{set}+1\right)}\right) \end{aligned} \tag{9}$$

where Q is the cumulative probability density function at the tail of standard normal distribution and N_{set} is the number of fault subsets; PFA is the average allocated to each fault subset in the traditional ARAIM algorithm, and the continuity risk is not assigned with no fault. Therefore, $K_{fa,0} = 0$. According to **Eq. 1**, the VPL is determined by the maximum function, and the average distribution of $PHMI$ and PFA is not the optimal distribution strategy. According to **Eq. 3**, the VPL can be reduced by optimizing continuity risk PFA and integrity risk PHMI.

Allocating Probability of Hazardously Misleading Information and Probability of False Alarm Based on the Particle Swarm Optimization Algorithm

1) Selection of Fitness Function

According to **Eqs 1–9**, the calculation method of the VPL corresponding to fault subset k can be expressed as follows:

$$\begin{aligned} VPL_k = &-Q^{-1}\left(\frac{PFA}{N_{\mathrm{set}}}\right) \times \sigma_{\mathrm{dv},k} + \Bigg(\\ &- Q^{-1}\left(\frac{PHMI}{P_{\mathrm{sat},i}\left(N_{\mathrm{set}}+1\right)}\right) \times \sigma_{\mathrm{v},k} \Bigg) + \sum_{i=1}^{N_{\mathrm{sat}}} |S_k(3,i)| \times b_{\mathrm{nom},i} \\ &+ \sum_{i=1}^{N_{\mathrm{sat}}} |\triangle S_k(3,i)| \times b_{\mathrm{cont},i} \end{aligned} \tag{10}$$

When the PSO algorithm is combined with the allocation process of $PHMI$ and PFA, a reasonable optimization objective, fitness function, should be selected. According to the above **Eq. 10**, the VPL is selected as the optimization target, and the integrity and continuity risk assigned to each fault subset are taken as the optimization parameters. The optimization targets are set as follows:

$$\begin{aligned} &min\ max\left(VPL_k\left(PHMI_k, Pfa_k\right)\right) \\ &s \cdot t \cdot \begin{cases} \sum_{k=1}^{N_{\mathrm{set}}} P_{\mathrm{HMI},k} \le PHMI \\ \sum_{k=1}^{N_{\mathrm{set}}} P_{\mathrm{fa},k} \le Pfa \end{cases} \end{aligned} \tag{11}$$

where $P_{HMI,k}$ is the integrity risk assigned to the fault subset k and $P_{\mathrm{fa},k}$ is the continuity risk assigned to the fault subset k. Ideally, the VPL corresponding to each fault subset is the same. Therefore, the calculation of the optimization objective can be expressed as follows:

$$VPL = min VPL_k\left(k = 0, \ldots, N_{\mathrm{set}}\right) \tag{12}$$

Definition:

$$D_k = \sum_{i=1}^{N_{\mathrm{sat}}} |S_k(3,i)| \times b_{\mathrm{nom},i} + \sum_{i=1}^{N_{\mathrm{sat}}} |\triangle S_k(3,i)| \times b_{\mathrm{cont},i} \tag{13}$$

Therefore, the VPL corresponding to each fault subset is expressed as:

$$VPL_k = K_{\mathrm{fa},k} \times \sigma_{\mathrm{dv},k} + K_{\mathrm{md},k} \times \sigma_{\mathrm{v},k} + D_k \tag{14}$$

In order to obtain a unique solution, according to the multi-objective optimization theory, transforming multi-objective optimization into single-objective optimization, and the weighted sum of VPL_k is taken as the optimization objective:

$$\begin{aligned} &min\ F \\ &\begin{cases} F_k = \sum_{k=0}^{N_{\mathrm{set}}} g_k \times VPL_k \\ g_k = \dfrac{\left(\sigma_{\mathrm{dv},k} + \sigma_{\mathrm{v},k}\right)}{\sum_{k=0}^{N_{\mathrm{set}}} \sigma_{\mathrm{dv},k} + \sum_{k=0}^{N_{\mathrm{set}}} \sigma_{\mathrm{v},k}} \\ VPL_k = K_{\mathrm{fa},k} \times \sigma_{\mathrm{dv},k} + K_{\mathrm{md},k} \times \sigma_{\mathrm{v},k} + D_k \end{cases} \end{aligned} \tag{15}$$

2) PHMI and PFA Allocation Optimization Method

The PSO algorithm is introduced into the allocation process of integrity and continuity risk; the detailed steps are as follows:

Step 1. Initialize the algorithm parameters;

Step 2. Form the initial population; according to the number of fault subsets N_{set}, generate M groups' random number, both from 0 to $PHMI$ and from 0 to PFA, and form the initial population G_{0m}:

$$\boldsymbol{G}_{0m} = \begin{bmatrix} PHMI_{m0}, PHMI_{m1}, \ \ldots \ , & PHMI_{mN_{\text{set}}} \\ 0 \ , & Pfa_{m1}, Pfa_{m2}, \ldots, Pfa_{mN_{\text{set}}} \end{bmatrix} \tag{16}$$

where $m = 1, \ldots,$ M,M is the number of populations, and there exists:

$$\begin{cases} \sum_{k=0}^{N_{\text{set}}} P_{\text{HMI},mk} \le PHMI \\ \sum_{k=1}^{N_{\text{set}}} P_{\text{fa},mk} \le Pfa \end{cases} \tag{17}$$

Step 3. Calculate fitness function: according to the fitness function $min\ F$ selected above, each particle in the initial population is substituted into the fitness function, and the fitness value corresponding to each particle is calculated, and the particle position with the minimum fitness value is set as the initial global optimal position $gbest$, and then the position of each particle itself is set as the initial individual position $pbest_m$. The updated velocity of the particle is as shown in **Eq. 18**, and the updated position of the particles is as shown in **Eq. 19**.

$$\boldsymbol{v}_m(t+1) = \omega v_m(t) + c_1 r_1 \left(pbest_m - \boldsymbol{x}_m(t)\right) + c_2 r_2 \left(gbest - \boldsymbol{x}_m(t)\right) \tag{18}$$

$$\boldsymbol{x}_m(t+1) = \boldsymbol{x}_m(t) + \boldsymbol{v}_m(t+1) \tag{19}$$

where ω is the inertia weight factor, c_1 and c_2 are the positive acceleration constants, r_1 and r_2 are the random number of the average distribution between 0 and 1, and $\boldsymbol{v}_m$ represents the moving speed of the m particle.

The selection of parameter values affects the performance of the PSO algorithm. Based on the research of Shi and Cler et al., many simulation experiments are carried out. The PSO algorithm parameters are set up: the population particle size M = 50; the maximum iteration times $M_t = 50$; the acceleration coefficient $c_1 = c_2 = 1.2$, the maximum particle moving speed $v_{\max} = 4$, and the minimum moving speed $v_{\min} = -1$; and the inertia weight factor is introduced into the adaptive value as **Eq. 20**.

$$\omega = \omega_{\max} - (\omega_{\max} - \omega_{\min})\frac{t}{M_t} \tag{20}$$

where t is the number of iterations and $pbest_m$ and $gbest_m$ are the maximum and minimum inertia coefficients, respectively.

Step 4. Iterative updating: by judging the individual optimal value of each particle in the initial iteration, the individual optimal position $pbest_m$ passed by each particle and the global optimal position $gbest$ in the population are determined during each iteration (Wang S. Z. et al., 2021). Each particle gets the $gbest$ and $pbest_m$ according to the last iteration, updates its own position and velocity based on **Eqs 18–20**, then the algorithm calculates the fitness value corresponding to the updated position until the conditions of each particle are met, and the optimized allocation strategy and VPL are obtained.

TABLE 1 | ISM parameter settings.

Group	Constellation	p_{sat}	p_{const}	b_{cont}	b_{nom}	σ_{URA}	σ_{URE}
1	GPS	10–5	10–8	0	3/4	1	2/3
	BDS	10–4	10–8	0	3/4	1	2/3
2	GPS	10–4	10–8	0	3/4	1	2/3
	BDS	10^{-5}	10^{-8}	0	3/4	1	2/3
3	GPS	10^{-5}	10^{-8}	0	3/4	3/2	1
	BDS	10^{-4}	10^{-8}	0	3/4	1	2/3

EXPERIMENTAL RESULTS AND ANALYSIS

In order to verify the performance of the algorithm, BDS/GPS dual-constellation was first adopted, and the simulation time was 3 h. Three groups of parameters are set within the range for ISM parameters, as shown in **Table 1**. As for the prior probabilities P_{sat} and P_{const}, their work is based on GPS commitment and observation of historical data. The satellite fault probability and the constellation fault probability are deduced by massive data. In this section, it was decided to vary the probability of fault between 10^{-4} and 10^{-5} to show the impact on the fault modes and associated performance. Global availability of ARAIM coverage is expressed as the percentage of total users with a service availability ratio of more than 99.5% during the simulation period.

For the area covered by ARAIM, the ratio of the available time of ARAIM to the total simulation time is used to make the contour plot. Under three groups of parameters, the global VPL and availability of ARAIM between the traditional PHMI and PFA allocation and PSO-based PHMI and PFA allocation method are shown in **Figures 1–3**.

Figures 1–3 show the global VPL and availability of ARAIM between the traditional method and optimized method by BDS/GPS dual-constellations under different ISM parameters. Each set of results on the left corresponds to the traditional allocation method in every figure's (a) and (b); the other side corresponds to the proposed optimization algorithm. As can be seen from **Figures 1** and **4**, in the traditional allocation method, the VPL of some ARAIM user areas is greater than VAL. However, in the optimized algorithm, the VPL of the corresponding part of the area is optimized to be less than VAL to meet the LPV-200 service requirement. For example, in **Figure 1A**, the area near the prime meridian and below 60°S; in **Figure 2A**, the area near 20–60°S and 0–100°E; and in **Figure 3A**, the area near 20–60°S and 0–100°W. Analyzing the availability of ARAIM corresponding to the above region can lead to the conclusion that the larger the VPL

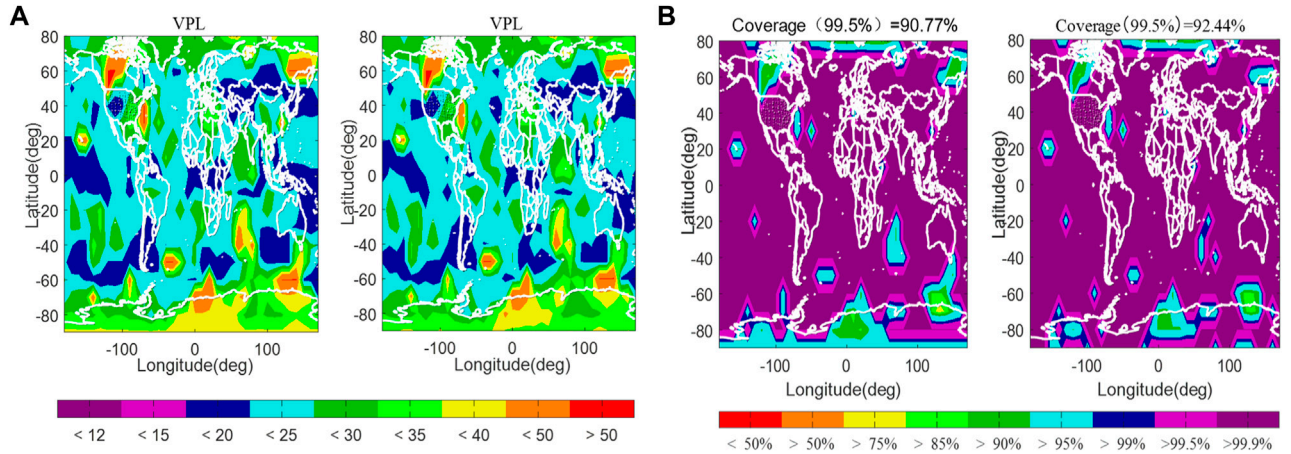

FIGURE 1 | Global VPL and ARAIM global availability under the first set of parameters. **(A)** Global VPL corresponding to the two allocation methods under the first set of parameters. **(B)** Global availability of ARAIM corresponding to the two allocation methods under the first set of parameters.

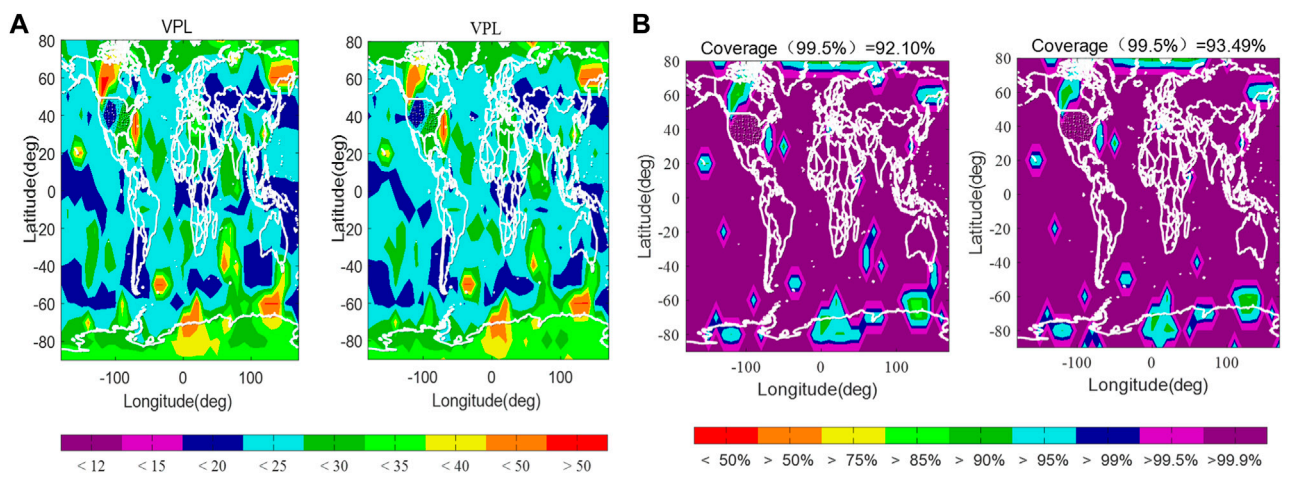

FIGURE 2 | Global VPL and ARAIM global availability under the second set of parameters **(A)** Global VPL corresponding to the two allocation methods under the second set of parameters. **(B)** Global availability of ARAIM corresponding to the two allocation methods under the second set of parameters.

corresponding to the traditional allocation method, the more obviously the algorithm proposed optimizes the VPL, and the more obvious the improvement in the ARAIM availability coverage in the corresponding region. Therefore, the optimization algorithm can reduce the VPL of the ARAIM user area and improve the availability of ARAIM coverage in the corresponding area. **Table 2** compares the global availability of ARAIM corresponding to the two allocation methods under four groups of parameters.

Table 2 and **Figures 1**–**3** show that the optimized allocation method can improve the global availability coverage of ARAIM. The VPL is larger, so the optimization effect of the algorithm will be better. If the availability of ARAIM becomes higher and higher, the optimization effect of the improved algorithm will become smaller. The traditional MHSS ARAIM algorithm uses the average allocation method to allocate the probability of PHMI and PFA to each satellite. This traditional allocation mode is deduced by the GPS constellation model, and the GPS constellation satellites fault rate is low and constellation distribution is uniform. The calculated VPL shows little difference by various fault assumptions; the method can be used to calculate average distribution probability, and the result will not be affected by great error. However, for the multi-constellation GNSS based on BDS, the characteristics of the BDS constellation are different from those of the GPS constellation, and the allocation of the BDS constellation is not uniform. It is different from the GPS constellation dominated by medium Earth orbit (MEO) satellites. The BDS constellation is composed of three kinds of orbits including GEO, MEO, and IGSO. The BDS satellites are distributed in three

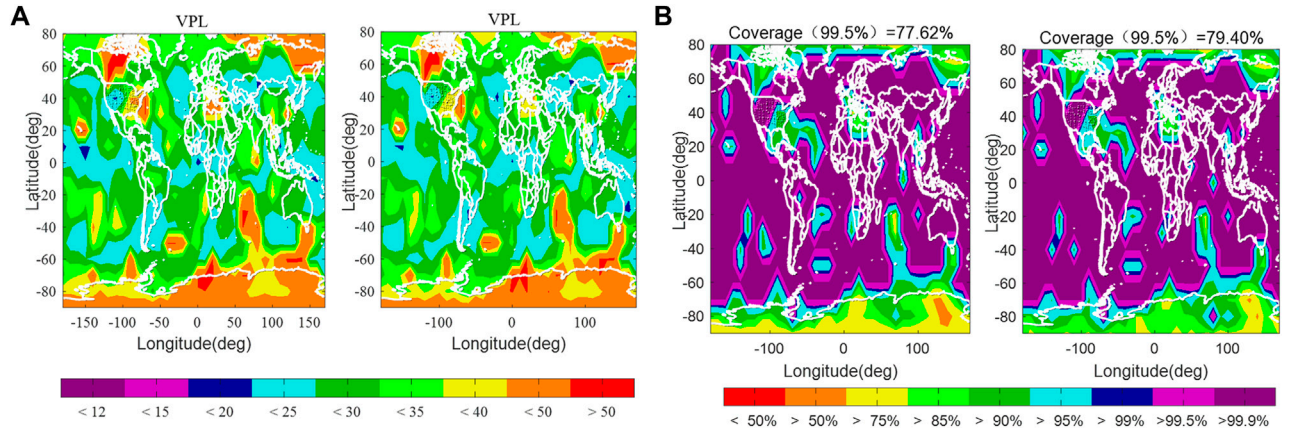

FIGURE 3 | Global VPL and ARAIM global availability under the third set of parameters. **(A)** Global VPL corresponding to the two allocation methods under the third set of parameters. **(B)** Global availability of ARAIM corresponding to the two allocation methods under the third set of parameters.

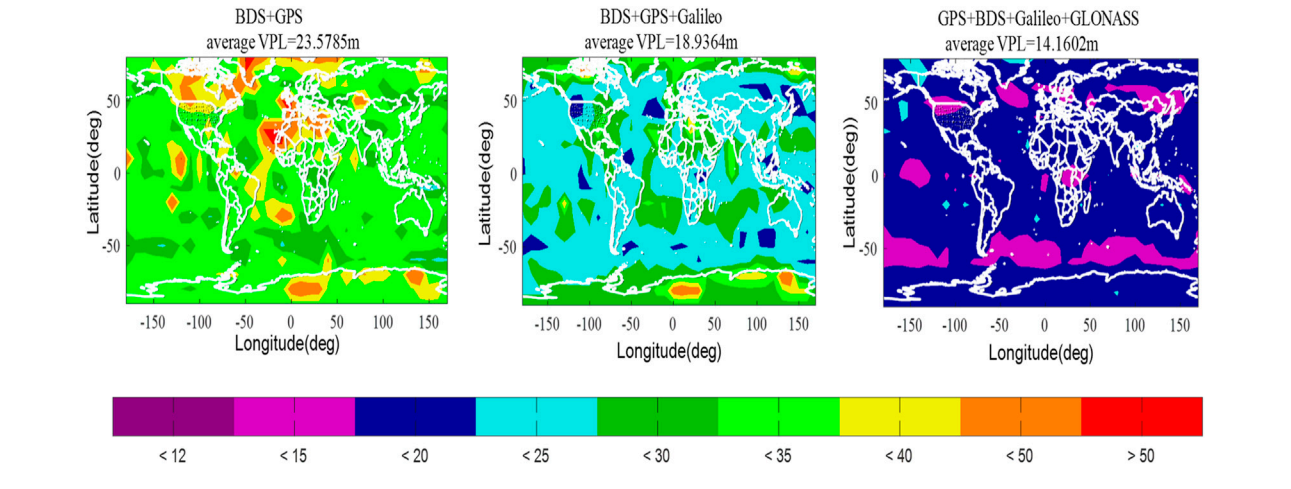

FIGURE 4 | VPL under different constellation numbers before optimization.

TABLE 2 | Global availability comparison between the traditional algorithm and the optimized algorithm.

Group	Traditional algorithm (%)	Optimized algorithm (%)
1	90.77	92.44
2	92.10	93.49
3	77.62	79.40

different orbits. Therefore, different BDS satellites contribute to different positioning errors. Due to the differences in the geometric configuration and constellation of each satellite, it will lead to some extreme assumptions which will have a serious impact on the results while using the average allocation strategy. As a result, it will lead to an excessive VPL and reduce the availability of global ARAIM. In the traditional average allocation of PHMI, PHMI is allocated to each fault subset evenly. Therefore, the final total PHMI rate is always equal to the pre-allocated PHMI risk rate, and the maximum VPL is taken as the upper limit of protection level in the subset and limit of the user availability of ARAIM. However, the allocation methods of PHMI and PFA based on the PSO algorithm regard different risk allocation strategies as different particles, and the weighted sum of the VPL corresponding to the fault subset is taken as the optimization objective function to establish different optimal allocation strategies. Therefore, different PHMI and PFA are allocated to different satellites, and the actual total PHMI and PFA are reduced as much as possible so as to improve the availability of ARAIM algorithm by reducing the VPL. Using the average allocation algorithm, the integrity risk and continuity risk are equally allocated to each fault subset, and the maximum VPL in the subset is taken as the upper limit of the VPL, which limits the ARAIM availability. However, PHMI and PFA are constructed as particle populations by using a PSO optimization

TABLE 3 | ISM parameter settings of each constellation.

Constellation/ISM	p_{sat}	p_{cont}	b_{cont}	b_{nom}	σ_{URA}	σ_{URE}
BDS	10^{-4}	10^{-4}	0	1	1.2	4/5
GPS	10^{-5}	10^{-4}	0	3/4	1	2/3
Galileo	10^{-5}	10^{-4}	0	3/4	1	2/3
GLONASS	10^{-4}	10^{-3}	0	1	1.2	4/5

based on the ARAIM algorithm under more than two constellations, this section discusses the integrity requirements of different navigation areas and analyzes the availability of ARAIM under different allocation schemes for three constellations and four constellations under different integrity requirements (Li et al., 2017). The GEAS report showed that ARAIM TSG aims to realize ARAIM on the basis of dual-

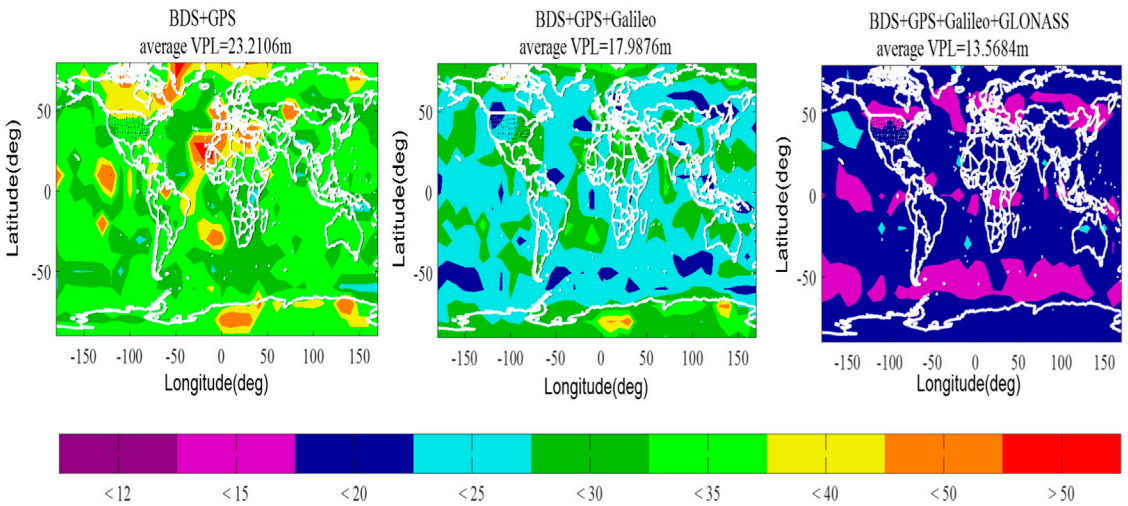

FIGURE 5 | VPL under different constellation numbers after optimization.

allocation strategy. PHMI and PFA were allocated to different satellites by the particle swarm optimization algorithm, total PHMI and PFA were reduced, and the ARAIM availability was improved by reducing the VPL. Meanwhile, **Table 2** and **Figures 1–3** show that within the appropriate range of ISM parameters, different satellite fault probabilities and URA have different effects on the global availability of ARAIM. Satellite fault probability has little influence on the global availability of ARAIM, and URA has a great influence on the availability of ARAIM.

MULTI-CONSTELLATION ADVANCED RECEIVER AUTONOMOUS INTEGRITY MONITORING AVAILABILITY ANALYSIS

The above section introduced the availability of the BDS/GPS dual-constellation VPL and ARAIM based on the PSO algorithm. The results show that the PHMI and PFA allocation scheme based on the PSO algorithm can achieve the purpose of optimizing the dual-constellation VPL and improve the availability of dual-constellation ARAIM. However, there are currently four-constellation operations to provide navigation services for aviation users, and the ARAIM algorithm with more than two constellations should be given priority consideration. In addition, the integrity requirements of different precision approach phases are different. Therefore, frequency (Liu et al., 2022; Li et al., 2020). Combined with the above reports and the literature (Blanch et al., 2015), according to the baseline ARAIM algorithm, the ISM parameters corresponding to BDS, GPS, GLONASS, and Galileo constellations are set within an appropriate range, as shown in **Table 3**. The different constellations are set, according to statistics, to the number of faults per year with 1-h mean time to alert (MTTA) by the ground segment. The VPL and the availability of the integrity algorithm under different constellation numbers are verified.

Figures 5 and **6** simulate the integrity algorithm according to the integrity requirements at different phases, and analyze the relationship between the constellation number and the VPL.

The results of the analysis in **Figure 5** show that the addition of constellations with GPS-equivalent performance to the traditional integrity algorithm significantly reduces the VPL of the integrity algorithm. When there are four constellations, VAL can achieve a high coverage rate of up to 15 m. But the results of the four constellations show that this method is still inadequate to meet the precise 10-m VAL required by CAT-I. **Figure 6** shows the VPL of the integrity algorithm optimized based on the PSO algorithm. Compared with the global average VPL value in the same constellation combination system, PHMI and PFA allocation schemes based on the PSO algorithm reduced the global average VPL by about 0.3 m in the BDS + GPS combination; in the case of BDS/GPS/Galileo, PHMI and PFA allocation strategies based on the PSO algorithm reduced the

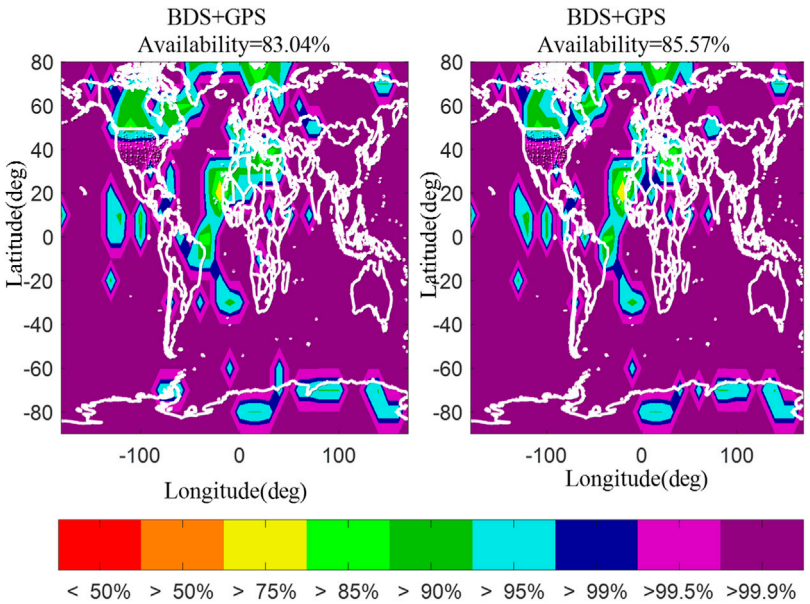

FIGURE 6 | Availability before and after dual-constellation optimization under the condition of VAL = 35 m.

global VPL by about 1 m. In BDS/GPS/Galileo/GLONASS, the PHMI and PFA sub-strategies based on the PSO algorithm reduce the VPL by about 0.5 m. In conclusion, PHMI and PFA allocation schemes based on the PSO algorithm can still achieve the optimization of the VPL in the case of different constellation combinations. As the number of constellations increases, the number of satellites increases gradually, and the VPL of multiple constellations decreases gradually.

4.1 Availability Analysis of the Multi-Constellation Global Navigation Satellite System's Integrity Monitoring Algorithm

In order to further verify the impact of the PHMI and PFA allocation scheme based on the PSO algorithm on the availability of the integrity algorithm under the combined system, this section discusses the integrity algorithm simulation analysis based on the integrity requirements of the different phases. During the vertical guidance approach phase and precision approach phases, which refers to the traditional PHMI before optimization and PFA scheme, the optimized means PHMI and PFA allocation scheme based on the PSO algorithm. For different allocation schemes, **Figures 6–10** show the availability of the integrity algorithm before and after optimization for different constellation combinations under different phases and different integrity requirements. Among them, 1) when the vertical alert limit (VAL) = 15 m, the availability coverage rate before and after dual-constellation and three-constellation optimization is 0%; 2) when the vertical alarm limit (VAL) = 20 m, the availability coverage rate before and after dual-constellation optimization is 0%; 3) when the vertical alert limit (VAL) = 35 m, the availability coverage rate of the integrity algorithm before and after the four-constellation optimization is 100%. Therefore, under the above three conditions, the availability coverage of the integrity algorithm before and after optimization will not be analyzed in the following.

It can be seen from **Figure 6** that compared with the traditional algorithm, the optimized algorithm can improve the availability of dual-constellation by about 2.53% under LPV-200, and it can be found that the optimized algorithm is more obvious at the area near 60–80°S. It can also be found that the availability of ARAIM is different under different ISM parameters, and the optimized algorithm has different degrees of optimization. **Figure 7** shows availability before and after three-constellation optimization under the condition of VAL = 35 m. It can be seen from the figure that when the number of constellations increases, the availability of the ARAIM algorithm before and after optimization is improved to varying degrees.

4.2 Analysis From the Constellation Number

Analyzing **Figures 6** and **10**, at the same phase of integrity requirement, the increase of constellation number can significantly improve the availability coverage of the integrity algorithm. When the VAL = 35 m, the availability coverage of the integrity algorithm of the dual-constellation BDS/GPS is about 10% less than that of the three-constellation BDS/GPS/Galileo. When the VAL = 20 m, the availability coverage of the integrity algorithm under the four-constellation BDS/GPS/Galileo/GLONASS is about 80% higher than the availability coverage of the integrity algorithm under the three-constellation BDS/GPS/Galileo. When the VAL = 15 m, only the availability of the integrity algorithm under four constellations is greater than 0%. As can be seen from **Figures 5** and **6**, when VAL = 35 m, the VPL

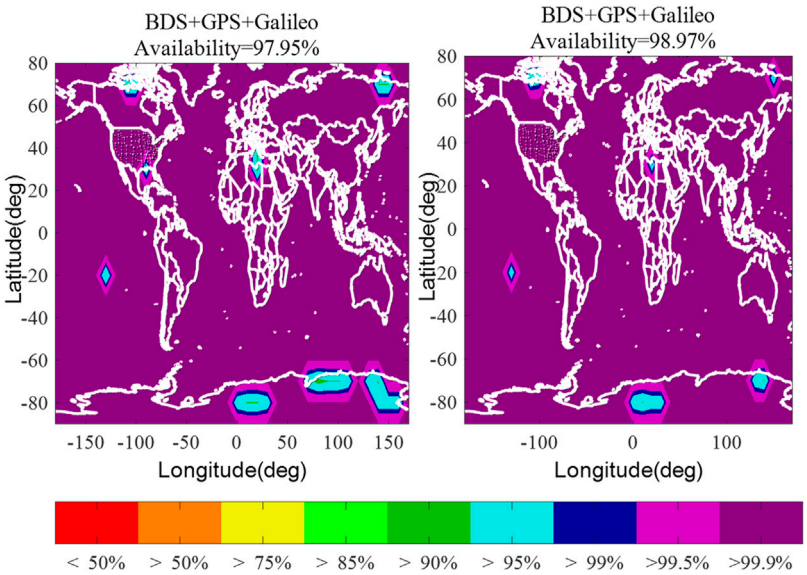

FIGURE 7 | Availability before and after three-constellation optimization under the condition of VAL = 35 m.

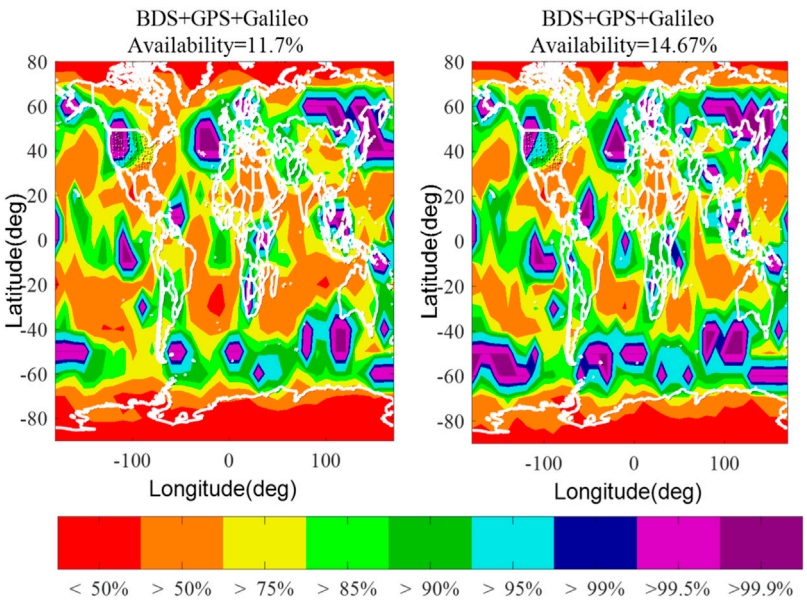

FIGURE 8 | Availability before and after three-constellation optimization under the condition of VAL = 20 m.

of BDS/GPS, BDS/GPS/Galileo, and BDS/GPS/Galileo/GLONASS before and after optimization is mostly less than 35 m; when VAL = 20 m, the VPL of BDS/GPS/Galileo by a very small percentage is less than 20, so the three constellations meet the availability of less than 20% at VAL = 20 m. However, the VPL of the four constellations is above 20; when VAL = 15 m, it can be found that the VPL is a little less than 15 for the double and three constellations. The availability of ARAIM for the four constellations can reach around 24%. Based on the above analysis, the availability of the ARAIM algorithm before and after optimization for the same constellation combination is presented in **Tables 4** and **5**.

Tables 4 and **5** show that as the number of constellations increases, the availability coverage of the integrity algorithms is also increased, and the integrity algorithm under four constellations can meet the integrity requirements of a more stringent phase. Using the new method can improve the global availability in different navigation phases. Aiming at dual

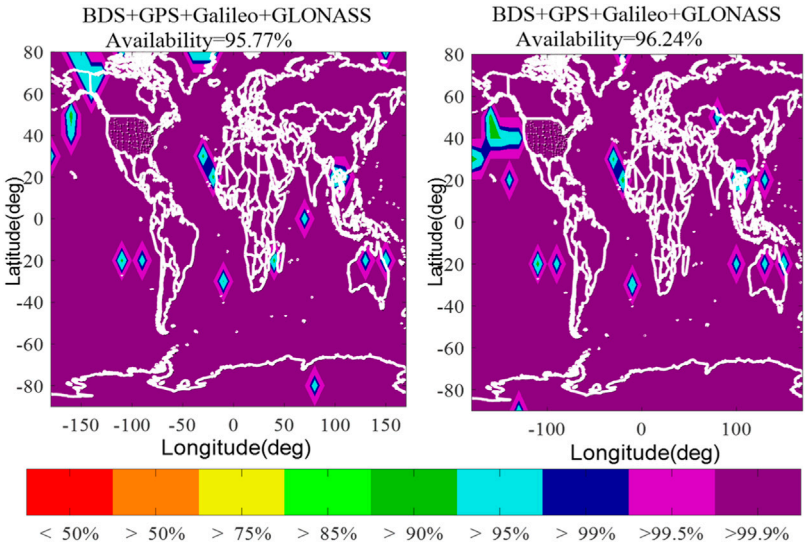

FIGURE 9 | Availability before and after four-constellation optimization under the condition of VAL = 20 m.

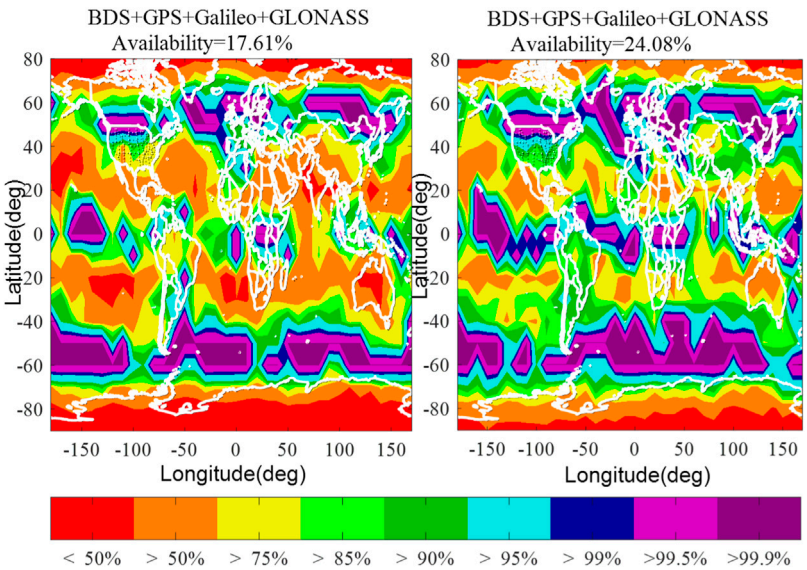

FIGURE 10 | Availability before and after four-constellation optimization under the condition of VAL = 15 m.

TABLE 4 | Availability analysis of the multi-constellation integrity algorithm before optimization.

VAL(m)	Dual constellations (%)	Three constellations (%)	Four constellations (%)
15	0	0	17.61
20	0	11.7	95.77
35	83.04	97.95	100

constellations, VAL = 35 m can improve the availability obviously, and the new algorithm is improved about 2.53%; aiming at three constellations, VAL = 20 m can improve the availability obviously, and the new algorithm is improved about 2.97%; and aiming at four constellations, VAL = 15 m can improve availability obviously, and the new algorithm is

TABLE 5 | Availability analysis of the optimized multi-constellation integrity algorithm.

VAL(m)	Dual constellations (%)	Three constellations (%)	Four constellations (%)
15	0	0	24.08
20	0	14.67	96.24
35	85.57	98.97	100

improved about 6.47%. In addition, the improved PHMI and PFA allocation schemes based on PSO can improve the availability of integrity algorithms to a certain extent. When comparing the same vertical alarm limit and the different constellation combinations, it can be found that the optimized algorithm can better meet the requirements of completeness than the traditional algorithm in different phases of navigation with the increase of the number of constellations.

4.3 Analysis of Complexity of an Algorithm

The complexity of an algorithm is the basic method to measure the efficiency of an algorithm. The time complexity of an algorithm is usually expressed using big "O" notation. The time complexity of the algorithm is also the time metric of the algorithm, denoted as $T(n) = O(f(n))$. n is the size of the problem. It means that as the size of the n problem increases, the growth rate of the algorithm execution time is the same as the growth rate $f(n)$ of the algorithm, which is called the asymptotic time complexity of the algorithm. By using the "big O-order" calculation step to calculate the traditional algorithm, the complexity can be obtained as $T(n) = O(n)$. The complexity of the improved algorithm is $T(n) = O(n^2)$. Aiming at the PSO algorithm, the time complexity is calculated by the number of particles, the number of iterations, and the time required for each iteration. Different parameter selection of the PSO algorithm will have a certain influence on the complexity of the algorithm. In terms of the complexity, it can be seen that the complexity of the traditional algorithm is better than that of the improved algorithm. Moreover, under the condition of the required alarm time for navigation performance, the improved algorithm can improve the global availability.

5 CONCLUSION

Advanced RAIM (ARAIM) technology is being developed as an aircraft-based augmentation system (ABAS) for use under multi-constellation operations. In this article, the PSO method is proposed to allocate the PHMI and PFA parameters of the ARAIM algorithm. The proposed algorithm is verified under BDS/GPS, BDS/GPS/Galileo, and BDS/GPS/Galileo/GLONASS multi-constellation, respectively. The experiment results demonstrate that the optimization algorithm proposed can reduce the VPL of the area covered by ARAIM. The optimized algorithm can also improve the global availability coverage of ARAIM under multi-constellation during the approach phase. Moreover, it can be shown that with the increasing number of satellites under multi-constellation, the availability of ARAIM globally is gradually improved. In the study, the results are instructive for the study of civil aviation navigation integrity monitoring. In addition, the optimized algorithm can easily fall into the local optimal solution, and it still needs to be improved in future work.

DATA AVAILABILITY STATEMENT

The data are available from the International GNSS Service at the following web locations: ftp://ftp.igs.org/pub/station/general/ ftp://ftp.igs.orggnsswhu.cn/pub/station/general/.

AUTHOR CONTRIBUTIONS

EW researched the advanced RAIM method. WS validated the results and undertook writing. XD researched particle swarm optimization algorithm. ZW revised the written work. SX analyzed the experimental results. HW investigated the related work.

FUNDING

This study was supported by the National Natural Science Foundation of China (62173237), the Open Fund of Key Laboratory of Flight Techniques and Flight Safety, CAAC (FZ2021KF15, FZ2021ZZ06), the Key R&D projects of Liaoning Province (2020JH2/10100045), the Zhejiang Key laboratory of General Aviation Operation technology (JDGA2020-7), and the Talent Project of Revitalization Liaoning (XLYC1907022).

REFERENCES

Bang, E., Milner, C., and Macabiau, C. (2020). Cross-correlation Effect of ARAIM Test Statistic on False Alarm Risk[J]. *GPS Solutions* 24 (4), 1–14. doi:10.1007/s10291-020-00997-w

Bang, E., and Milner, C. (2021). Integrity Risk under Temporal Correlation for Horizontal ARAIM. *IEEE Trans. Aerosp. Electron. Syst.* 57 (6), 3974–3987. doi:10.1109/taes.2021.3082665

Bang, E., Milner, C., Macabiau, C., and Estival, P. (2018). "ARAIM Temporal Correlation Effect on PHMI[C]," in Proceedings of the 31st International Technical Meeting of the Satellite Division of The Institute of Navigation, 2682–2694.

Blanch, J., Walker, T., Enge, P., Lee, Y., Pervan, B., Rippl, M., et al. (2015). Baseline Advanced RAIM User Algorithm and Possible Improvements. *IEEE Trans. Aerosp. Electron. Syst.* 51 (1), 713–732. doi:10.1109/taes.2014.130739

Blanch, J., Walter, T., Enge, P., Lee, Y., Pervan, B., et al. (2012). "Advanced RAIM User Algorithm Description: Integrity Support Message Processing, Fault Detection, Exclusion, and Protection Level Calculation[C]," in Proceedings of the 25th International Technical Meeting of The Satellite Division of the Institute of Navigation, 2828–2849.

Blanch, J., Walter, T., and Enge, P. (2014). Optimal Positioning for Advanced RAIM[J]. *J. Inst. Navigation* 60 (4), 279–289.

Chang, J., Zhan, X., Zhai, Y., Wang, S., and Lin, K. (2021). Analysis of BDS GEO Satellite Multipath Effect for GNSS Integrity Monitoring in Civil Aviation. *As* 4 (2), 133–141. doi:10.1007/s42401-020-00074-7

El-Mowafy, A., and Yang, C. (2016). Limited Sensitivity Analysis of ARAIM Availability for LPV-200 over Australia Using Real Data. *Adv. space Res.* 57 (2), 659–670. doi:10.1016/j.asr.2015.10.046

Joerger, M., and Pervan, B. (2016). Fault Detection and Exclusion Using Solution Separation and Chi-Squared ARAIM. *IEEE Trans. Aerosp. Electron. Syst.* 52, 726–742. doi:10.1109/taes.2015.140589

Joerger, M., and Pervan, B. (2020). Multi-constellation ARAIM Exploiting Satellite Motion. *Navigation* 67 (2), 235–253. doi:10.1002/navi.334

Kropp, V., Eissfeller, B., and Berz, G. (2014). "Optimized MHSS ARAIM User Algorithms: Assumptions, Protection Level Calculation and Availability Analysis[C]," in In 2014 IEEE/ION Position, Location and Navigation Symposium-PLANS 2014 (IEEE), 308–323.

Li, L., Wang, H., Jia, C., Zhao, L., and Zhao, Y. (2017). Integrity and Continuity Allocation for the RAIM with Multiple Constellations. *GPS Solut.* 21 (4), 1503–1513. doi:10.1007/s10291-017-0627-4

Li, R., Zheng, S., Wang, E., Chen, J., and Feng, S. (2020). Advances in BeiDou Navigation Satellite System (BDS) and Satellite Navigation Augmentation Technologies[J]. *Satell. Navig.* 1 (1), 1–23. doi:10.1186/s43020-020-00010-2

Liu, N., Wu, L., Wang, J., Wu, H., Gao, J., and Wang, D. (2022). Seismic Data Reconstruction via Wavelet-Based Residual Deep Learning. *IEEE Trans. Geosci. Remote Sens.* 60 (2), 1–13. doi:10.1109/tgrs.2022.3152984

Mei, H., Zhan, X., and Zhang, X. (2017). "GNSS Vulnerability Assessment Method Based on ARAIM User Algorithm[C]," in 2017 Forum on Cooperative Positioning and Service (CPGPS), 111–115.

Meng, Q., Liu, J., Zeng, Q., Feng, S., and Xu, R. (2019). Improved ARAIM Fault Modes Determination Scheme Based on Feedback Structure with Probability Accumulation[J]. *GPS Solutions* 23 (1), 1–11. doi:10.1007/s10291-018-0809-8

Sun, Y., Wang, T., Wang, Z., and Zhang, Z. (2015). "Optimal Risk Allocation for BDS/GPS Advanced Receiver Autonomous Integrity Monitoring[C]," in Proceedings of the 2015 (International Technical Meeting of The Institute of Navigation), 687–695.

Wang, E., Sun, C., Wang, C., Qu, P., and Huang, Y. (2021). A Satellite Selection Algorithm Based on Adaptive Simulated Annealing Particle Swarm Optimization for the BeiDou Navigation Satellite System/Global Positioning System Receiver[J]. *Int. J. Distributed Sens. Netw.* 17 (7), 1–14. doi:10.1177/15501477211031748

Wang, E., Yang, D., and Hong, C. (2019). Research Progress of ARAIM Technology[J]. *Telecommun. Sci.* 35 (8), 128–138.

Wang, E., Yang, D., Wang, C., Huang, Y., Qu, P., and Pang, T. (2020). Optimized Fault Detection Algorithm Aided by BDS Baseband Signal for Train Positioning. *Chin. J. electron.* 29 (1), 34–40. doi:10.1049/cje.2019.09.004

Wang, S. Z., Zhai, Y. W., and Zhan, X. Q. (2021). Characterizing BDS Signal-In-Space Performance from Integrity Perspective[J]. *Navigation - J. Inst. Navigation* 68 (2), 157–183. doi:10.1002/navi.409

Working Group C, EU-U.S (2017). *ARAIM Concept of Operation*. Washington, D.C: Federal Aviation Administration, 1–7. Available at: https://portal.icao.int/nsp/meetingdocuments/NSP4-10-20-October2017/NSP4_ip18_ HARAIMConOps-final.docx."

Working Group C, EU-U.S (2016). *ARAIM Technical Subgroup Milestone 3 Report*. Washington, D.C: Federal Aviation Administration, 73–97. Available at: https://www.gps.gov/policy/cooperation/europe/2016/working-group-c/ARAIM-milestone-3-report.pdf.

Yi, X., Zhu, A., and Yang, S. X. (2022). MPPTM: A Bio-Inspired Approach for Online Path Planning and High-Accuracy Tracking of UAVs. *Front. Neurorobot.* 15, 798428. doi:10.3389/fnbot.2021.798428

Zhai, Y., Zhan, X., and Chang, J. (2019b). An Integrated Fault Detection and Exclusion Scheme to Support Aviation Navigation. *As* 3 (1), 29–39. doi:10.1007/s42401-019-00039-5

Zhai, Y., Zhan, X., Chang, J., and Pervan, B. (2019c). "ARAIM with More Than Two Constellations[C]," in Proceedings of the ION 2019 Pacific PNT Meeting, 925–941.

Zhai, Y., Zhan, X., Joerger, M., and Pervan, B. (2019a). Impact Quantification of Satellite Outages on Air Navigation Continuity. *IET Radar, Sonar amp; Navig.* 13 (3), 376–383. doi:10.1049/iet-rsn.2018.5376

Zhang, Y., Wang, L., and Fan, L. (2020). MHSS ARAIM Algorithm Combined with Gross Error Detection. *J. Geodesy Geoinformation Sci.* 3 (2), 36–44.

Zhao, P., Joerger, M., Liang, X., Pervan, B., and Liu, Y. (2021). A New Method to Bound the Integrity Risk for Residual-Based ARAIM. *IEEE Trans. Aerosp. Electron Syst.* 57 (2), 1378–1385. doi:10.1109/taes.2020.3040527

Conflict of Interest: The authors declare that the research was conducted in the absence of any commercial or financial relationships that could be construed as a potential conflict of interest.